

Electronic Supplementary Information

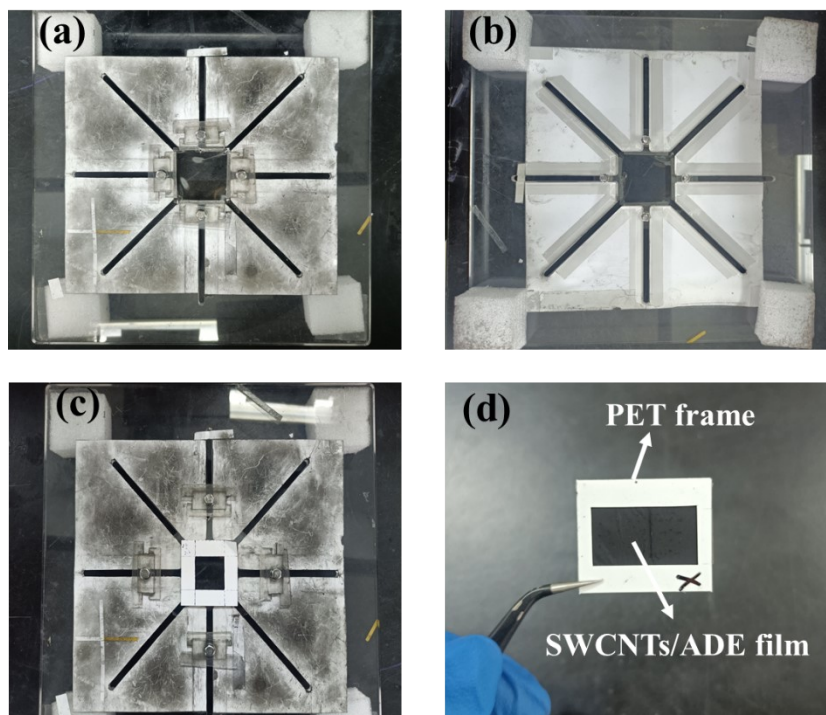
**Flexibly stretchable acrylic resin elastomer films for efficient electromagnetic
shielding and photothermal conversion**

*Ruoling Yu^a, Leilei Liang^b, Yue Zhao^a, Guangbin Ji^{*a}*

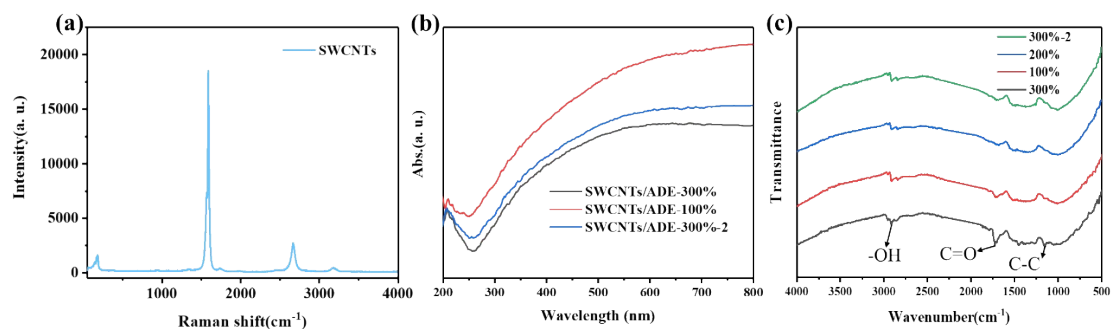
*^a College of Materials Science and Technology, Nanjing University of Aeronautics
and Astronautics, Nanjing 211100, P. R. China*

*^b School of Electronic Science and Engineering, Nanjing University, Nanjing 210093,
P. R. China*

**Corresponding Author: Prof. Dr. Guangbin Ji, E-mail: gbi@nuaa.edu.cn*



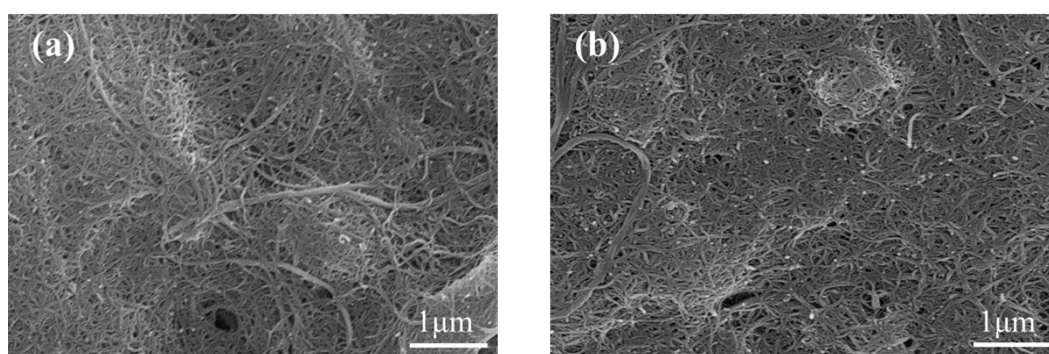
Supplementary Figure 1. Digital images of the top view **(a)** and bottom view **(b)** of the two-axis stretchable device. **(c)** Digital image of a two-axis stretchable device when sprayed with a custom sized mask. **(d)** Digital images of SWCNTs/ADE films fixed with a polyethylene terephthalate (PET) rectangular frame.



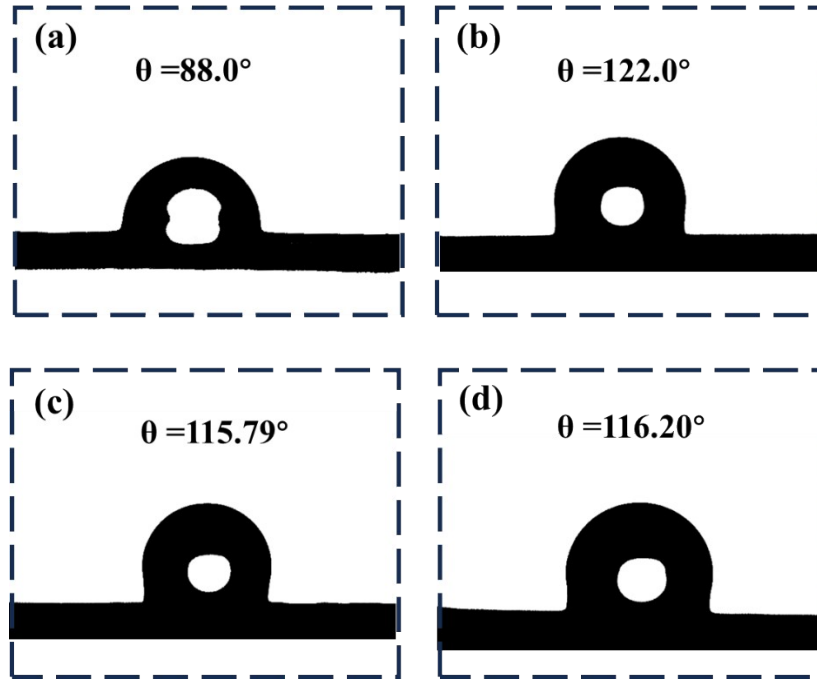
Supplementary Figure 2. **(a)** Raman spectra of pure single-walled carbon nanotube used in the experiment. **(b)** UV-Vis spectra of the SWCNTs/ADE films. **(c)** FTIR spectra of the SWCNTs/ADE films.

Due to the high purity of the single-wall carbon nanotube (SWCNTs), the content of amorphous carbon is very small, so the D-peak is not obvious. Because the degree of

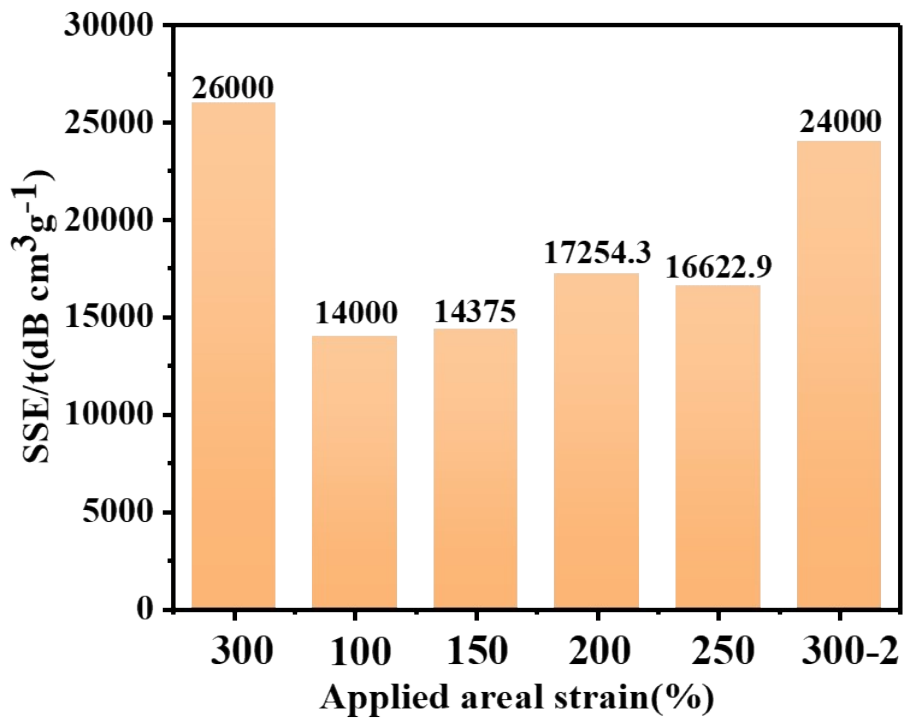
graphitization of SWCNTs is high, so the unsaturated functional groups in the carbon nanotubes are few, thus, the vibration of the -OH peak at 2913 cm^{-1} and the C=O peak at 1726 cm^{-1} is caused by the unsaturated functional groups in the acrylic resin substrate. The highest absorption of SWCNTs/ADE films at $8.6\text{ }\mu\text{m}$ was due to the C-C peak absorption at 1152 cm^{-1} , which resulted in the C-C bond in the conductive layer of SWCNTs.



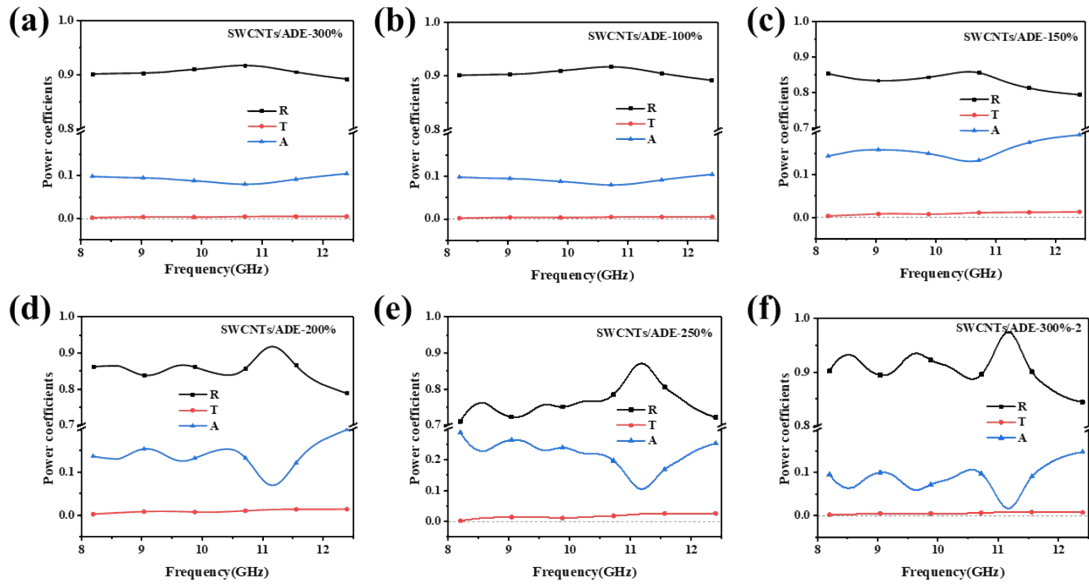
Supplementary Figure 3. SEM images of the SWCNTs distributed randomly and evenly on the ADE substrate of (a) 300% areal strain and (b) 100% areal strain.



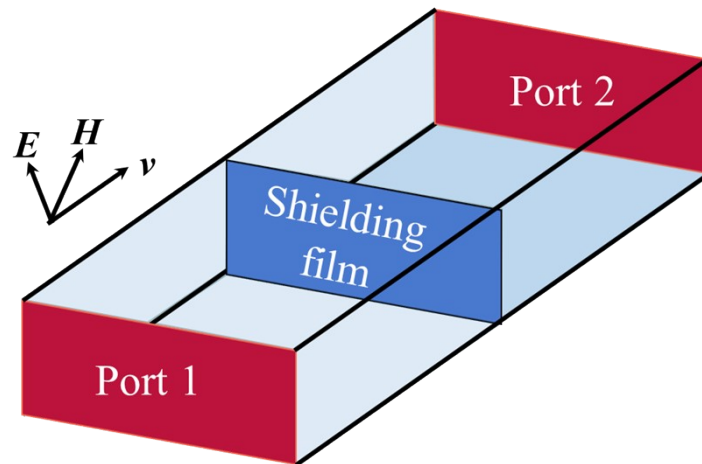
Supplementary Figure 4. (a) Digital image of water contact angle of the blank VHB film. Digital images of water contact angles of SWCNTs/ADE films at different applied areal strains: 150% (b); 250% (c); 300%-2 (d).



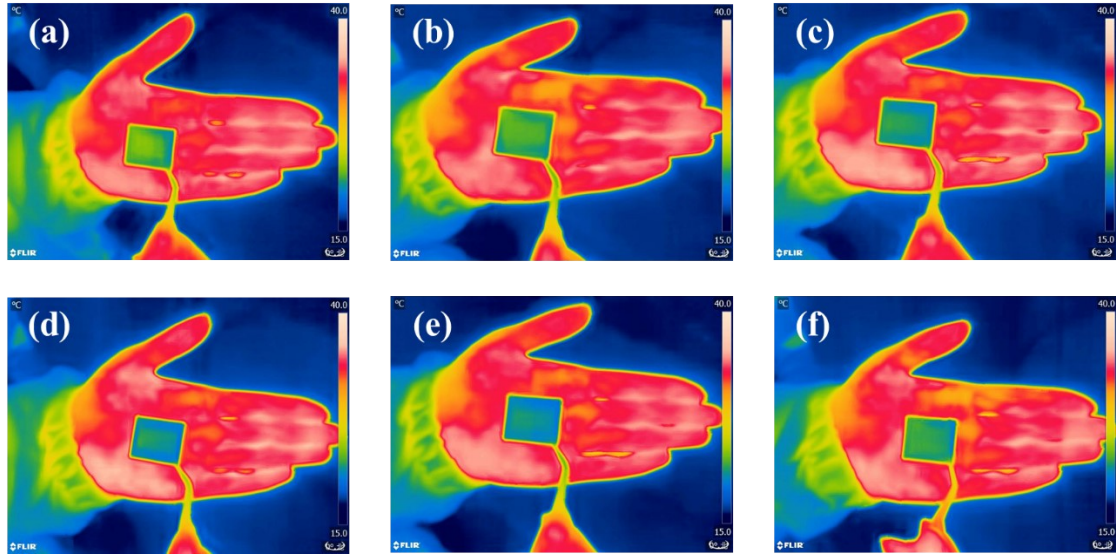
Supplementary Figure 5. SSE/t values of SWCNTs/ADE films under different applied areal strains.



Supplementary Figure 6. Power coefficients of SWCNTs/ADE films at different applied areal strains: 300% (a); 100% (b); 150% (c); 200% (d); 250% (e) and 300%-2 (f).



Supplementary Figure 7. The waveguide model for EMI shielding performance simulation.



Supplementary Figure 8. Infrared thermal images of SWCNTs/ADE films under different applied areal strains without heating: 300%(a); 100%(b); 150%(c); 200%(d); 250%(e); 300%-2(f).

Supplementary Table 1. Bending times and electromagnetic interference shielding efficiency.

Bending Cycles	Shielding efficiency (%)
0	99.9%
200	99.85%
400	99.6%
600	98.85%
800	98.03%
1000	96%